Ind. J. Pharm. Edu. Res., 2025; 59(4):1582-1602.
https://www.ijper.org

Original Article

In silico and *In vitro* Characterization of Potent CDK2 Inhibitors as Probable Cancer Therapeutics

Akram Ahmed Aloqbi*

Department of Biological Science, Faculty of Science, University of Jeddah, Jeddah, SAUDI ARABIA.

ABSTRACT

Background: Cyclin-Dependent Kinases (CDKs) are a family of serine/threonine protein kinases that play pivotal roles in the regulation of the cell cycle and various cellular processes. Among them, CDK2 is a crucial regulator of the G1/S phase transition and is crucial for the proper progression of the cell cycle. Dysregulation of CDK2 activity is frequently observed in various types of cancer, making it an attractive therapeutic target. Dinaciclib, a potent CDK2 inhibitor, has demonstrated clinical efficacy in the treatment of several malignancies. However, the development of novel CDK2 inhibitors with superior pharmacological properties remains an active area of research to improve therapeutic outcomes and address the limitations associated with existing agents. **Materials and Methods:** A comprehensive screening process began with the retrieval of 292 compounds from the PubChem database. The Lipinski rule of five was applied to narrow down the pool to 233 compounds with favorable drug-like properties. The selected compounds were then evaluated and compared to Dinaciclib using molecular docking and Molecular Dynamics (MD) simulations. *In vitro* assays were conducted to validate the inhibitory effect of lead molecule. **Results:** The computational analysis revealed that CID-23569275 emerged as the most promising lead compound. This compound exhibited higher LibDock scores, indicating stronger binding affinity towards CDK2 compared to Dinaciclib. MD simulations further demonstrated that CID-23569275 maintained greater conformational stability, as evidenced by their lower Root Mean Square Deviation (RMSD) and Root Mean Square Fluctuation (RMSF) values. Moreover, the combined evidence from the enzyme inhibition assay and fluorescence emission spectra strongly supports the effectiveness of CID-23569275 in inhibiting CDK2 activity. **Conclusion:** This comprehensive computational study has successfully identified CID-23569275 as potent lead compound for CDK2 inhibition, exhibiting superior pharmacological properties compared to the reference compound, Dinaciclib. The enhanced binding affinity and conformational stability of this lead candidate warrant its continued investigation through rigorous *in vitro* and *in vivo* studies to validate their therapeutic potential in cancer therapy.

Keywords: CDK2, Dinaciclib, Molecular Docking, Molecular Dynamics, ADMET, PubChem and Enzymatic assay.

Correspondence:
Dr. Akram Ahmed Aloqbi
Department of Biological Science, Faculty of Science, University of Jeddah, Jeddah-21589, SAUDI ARABIA.
Email: aaaloqbi@uj.edu.sa

Received: 15-12-2024;
Revised: 24-02-2025;
Accepted: 09-06-2025.

INTRODUCTION

Cyclin-Dependent Kinase 2 (CDK2) has emerged as an attractive anti-cancer drug target due to its key role in regulating cell cycle progression. Aberrant CDK2 activation is implicated in uncontrolled proliferation and genomic instability in numerous cancers.[1,2] Intensive efforts have focused on developing selective ATP-competitive small molecule CDK2 inhibitors as targeted therapeutics. First generation CDK inhibitors like flavopiridol demonstrated efficacy but lacked selectivity, leading to toxicity.[3] This spurred structure-guided design of selective CDK2 inhibitors, with dinaciclib being the first approved agent.[4] However, major challenges remain in optimizing CDK2 inhibitory potency and selectivity to progress beyond early clinical trials.[5] Advances in understanding structure-activity relationships have illuminated key structural determinants and binding dynamics governing CDK2 inhibition.[6,7] Integration of computational and experimental approaches offers promise to facilitate rational design of next-generation CDK2 targeted inhibitors, but further innovations are required to achieve clinical success.[8]

CDK2 is a serine/threonine kinase which associates with regulatory cyclins including cyclin E and cyclin A to orchestrate the G1/S and G2/M transitions during cell cycle progression.[9,10] CDK2 can phosphorylate critical substrates like Rb and E2F1 to activate E2F-dependent transcription and DNA synthesis in S phase.[11] Through complex formation with cyclin A2, CDK2 also mediates phosphorylation of WEE1, CDC25C and other key mitotic regulators to promote entry into mitosis.[12-14] Upregulated

DOI: 10.5530/ijper.20251532

CDK2-cyclin E activity occurs in many human cancers due to overexpression, amplification or defective degradation of cyclin E, and inactivation of endogenous CDK inhibitors like p21CIP1 and p27KIP1.[15,16] Hyperactive CDK2-cyclin E triggers unscheduled S phase entry, replication stress and genetic instability implicated in tumorigenesis.[17] Premature activation of CDK2 also contributes to deregulated G2/M and mitotic defects in cancer cells.[18] Hence, targeted inhibition of aberrant CDK2 signaling offers a potential differentiation strategy to halt uncontrolled proliferation in cancer versus normal cells.

Given its pro-oncogenic effects, CDK2 emerged as an attractive anti-cancer target decades ago. Early pan-CDK inhibitors like butyrolactone I, flavopiridol and roscovitine showed anti-proliferative efficacy against diverse cancer models but lacked selectivity, leading to dose-limiting toxicities.[19] This spurred structure-guided efforts to improve selectivity towards specific CDKs like CDK2 and CDK4/6.[20] Dinaciclib was the first selective CDK2 inhibitor to achieve FDA approval, demonstrating potent anti-tumor activity in preclinical studies.[21] Despite promise, dinaciclib showed limited single agent efficacy in early phase trials, though ongoing studies continue in combination regimens.[22] Other clinical CDK2 inhibitors like milciclib, SCH 727965 and SNS-032 showed initial responses but development was terminated due to lack of durable benefit or toxicity concerns.[23-25] A key challenge hampering progress is elucidating interactions governing binding selectivity and potency towards CDK2 versus other kinases.[8,26] Most inhibitors target the conserved ATP-site, but subtle structural differences can markedly impact selectivity.[6] Further research into CDK2 structure-activity relationships is vital to unlocking next-generation inhibitors.

Advances in elucidating CDK2 conformational dynamics and inhibitor interactions have provided insights to guide design of improved selective agents. High resolution X-ray crystal structures of CDK2-cyclin A complexes with diverse inhibitors revealed key binding determinants.[27,28] The CDK2 active site has a bi-lobed fold, with the N-terminal lobe comprised of a small β-sheet and α-helix known as the C-helix. The larger C-terminal lobe contains multiple α-helices and loops like the activation T-loop and PSTAIRE helix which undergo conformational changes upon cyclin binding.[29] ATP-competitive inhibitors occupy the cleft between the N and C-lobes. Hydrogen bonds with backbone atoms in the hinge region anchor inhibitors like the purine ring of dinaciclib.[30] Additional polar contacts and hydrophobic pockets like the gatekeeper site accommodate other moieties. However, the flat ATP-site topology hampers selectivity. Recent structural studies revealed an adjacent allosteric pocket which could confer selectivity if targeted.[31] Dynamics simulations illuminated rearrangements enabling inhibitor access to this pocket.[32] Beyond binding affinity, residence time linked to dissociation rate is emerging as a key parameter differentiating clinical candidates.[33] Approaches like tethering and proteolysis targeting chimera technology are elucidating dissociation kinetics to guide design.[34,35] Integration of such insights offers promise for addressing selectivity challenges.

While intensive efforts over decades have yielded CDK2 inhibitors entering early clinical evaluation, progress remains constrained by inadequate selectivity and efficacy. Advances in structural biology, computational modeling and biophysical techniques have revealed promising avenues to illuminate CDK2 conformational dynamics, structure-activity and structure-kinetics relationships to guide rational design of improved inhibitors. In particular, leveraging 3D receptor-ligand structural data through *in silico* approaches like molecular docking, dynamic simulations, binding free energy predictions and quantitative structure-activity relationships holds promise to accelerate selective lead discovery.[36-38] Integration of virtual screening, X-ray crystallography, NMR and biophysical assays represents a powerful structure-guided drug design paradigm for unlocking next-generation CDK2 agents with clinical potential.[39] Despite challenges ahead, continued technological and biological insights keep CDK2 inhibition at the forefront of targeted cancer therapy efforts.

MATERIALS AND METHODS

Software's and ligand library

Computational modeling was performed using Discovery Studio, a versatile software suite developed by BIOVIA (San Diego, CA) for molecular modeling and drug design applications.[40] Discovery Studio provides a comprehensive set of tools for structure optimization, binding site analysis, virtual screening, and prediction of pharmacokinetic properties to facilitate computational drug discovery efforts targeting proteins and other macromolecules.[41] For virtual screening of compound libraries, the LibDock module was utilized to efficiently dock ligands into the defined binding site and rank compounds based on calculated binding scores. LibDock employs optimized algorithms for rapid rigid docking and scoring to enable high-throughput *in silico* screening. Pharmacokinetic profiling of hit compounds was conducted using the ADME module in Discovery Studio, which calculates properties related to absorption, distribution, metabolism, excretion and toxicity. These *in silico* predictions provide valuable insights into the drug-likeness and pharmacokinetic behavior of compounds to guide lead prioritization and optimization. For small molecule ligands, three-dimensional structures were retrieved from the PubChem database,[42] which offers free access to over 96 million unique chemical structures and associated bioactivity data. By integrating flexible protein-ligand docking protocols with pharmacokinetic predictions and utilizing public compound databases, Discovery Studio enables efficient virtual screening and drug design workflows. The molecular dynamics portion was executed using. Desmond module of the Schrodinger Maestro

suite interface (Schrodinger release 2022-1, Desmond molecular dynamics system).

Data retrieval and Preparation

The X-ray crystal structure of human CDK2 in complex with the inhibitor dinaciclib (PDB ID 4KD1, 2.01 Å resolution) was obtained from the Protein Data Bank, the universal public archive of biomolecular structures. This high-resolution structure provided an ideal starting point for modeling the CDK2 ligand binding pocket and conducting virtual screening. Using the Discovery Studio modeling suite, the 4KD1 structure file was imported and prepared for docking by removing all crystallographic water molecules and the co-crystallized dinaciclib ligand. The binding site was mapped based on the spatial coordinates of dinaciclib from the crystal structure, in order to precisely define the active site region for docking experiments. To alleviate steric clashes and optimize the hydrogen bonding network, energy minimization was performed on the prepared CDK2 structure using the all-atom CHARMM36 force field.[43] This computational relaxation step serves to refine the protein structure by relaxing high energy conformations prior to docking.

A set of 3D small molecule inhibitors based on the structural similarity with Dinaciclib molecule were retrieved in SDF format from the PubChem database. This curated set of structurally similar CDK2 inhibitors was prepared for docking by adding implicit hydrogens and performing energy minimization using the Merck Molecular Force Field (MMFF94)[44] as implemented in Discovery Studio. Minimization generates low-energy conformations while retaining initial scaffold geometries.

Adsorption, Distribution, Metabolism, and Excretion and Toxicity prediction

In silico prediction of Absorption, Distribution, Metabolism, Excretion (ADME), and toxicity properties is an integral component of modern computational drug design workflows. The ADME module implemented in Discovery Studio was utilized to evaluate key molecular properties and pharmacokinetic parameters for the docked ligand hits obtained from virtual screening. Calculated aqueous solubility provides insight into absorption and formulation viability, while Caco-2 cell permeability and human intestinal absorption models predict gastrointestinal absorption and bioavailability. Plasma protein binding affinity and blood-brain barrier penetration were estimated to reveal distribution characteristics. Models of cytochrome P450 2D6 inhibition and hepatotoxicity were included to assess metabolic stability and potential for adverse effects. Additionally, the TOPKAT module of Discovery Studio was used to computationally profile Absorption, Distribution, Metabolism, Excretion, and Toxicity (ADMET) characteristics. TOPKAT employs statistically robust Quantitative Structure-Activity Relationship (QSAR) models trained on diverse empirical bioactivity datasets to predict mutagenicity, carcinogenicity, skin sensitization, and other toxicological endpoints.

By extensively evaluating ADME properties, binding, permeability, metabolic stability, and safety parameters, this computational profiling was performed to identify CDK2-targeted ligands with favorable pharmacokinetic and toxicity risk profiles to select optimal candidates for further experimental validation and drug development.

Molecular Docking

Molecular docking was performed using both the LibDock and CDOCKER modules within Discovery Studio to comprehensively evaluate ligand binding. LibDock functions by first mapping interaction hotspots on the receptor surface, then aligning ligands using these sites to guide orientation and minimize the energy of the complex using the CHARMm force field. The ligands were aligned within the defined CDK2 binding site using the hot spots to guide orientation. This efficient minimization algorithm precisely positions the ligand while maintaining the overall binding mode. Final scoring and ranking of the docked ligand complexes were based on the calculated LibDock scores, with higher values indicating more favorable predicted binding. Visual inspection of the top-scoring docked ligand poses provided insights into specific molecular interactions with key CDK2 active site residues. Poses were scored based on the calculated LibDock energy.

CDOCKER is an advanced docking method that adds in molecular dynamics simulations to refine and rescore the docked poses for greater accuracy. After the initial LibDock hotspot alignment, CDOCKER applied simulated heating and cooling to induce secondary structure changes in the receptor. The ligands were then redocked into this refined binding site and the CHARMM energy calculated. By integrating LibDock for rapid rigid docking with the more sophisticated CDOCKER protocol, robust screening and accurate binding affinity prediction was enabled. The docked complexes were analyzed by visualizing ligand poses and comparing scoring values to identify optimal CDK2 inhibitor candidates.

MD Simulation

It is critical to understand the inherent dynamics of macromolecules in living systems in both temporal and spatial dimensions. Understanding the quantum mechanical motion of macromolecules in living systems, including proteins, DNA, and other chemicals, across nanosecond time scales is made possible in large part by the molecular dynamics simulation technique. Thus, we used the academic version of the Desmond module of the Schrodinger Maestro suite interface (Schrodinger release 2022-1, Desmond molecular dynamics system) to run 50 ns MD simulations of our top lead against CDK2. The specifications of the device comprised a Linux workstation running Ubuntu 22.04

LTS OS (CPU=intel 12 generation core i5 12500h, 16GB memory, installed Nvidia GeForce RTX 3050 graphics card, and 512GB SSD card).

The protein preparation wizard module of the Schrodinger suite was used to initially prepare the particular complex after the complexes of the chosen molecule with the target were uploaded. After the complex was pre-processed, the prime license was used to create the missing side chains and loops. The protein was finally reduced and refined using force field OPLS_2005 after the polar hydrogen and terminal cap were introduced and the water molecules longer than 5Å from heteroatoms were removed. Additionally, the constructed system was covered by the Desmond system builder module inside an orthorhombic box with dimensions of X=10Å, Y=10Å, and Z=10Å, respectively. Long-range electrostatic interactions between molecules were computed using the particle mesh Ewald method. Temperature and pressure were controlled using the Martyna-Tuckerman-Klein chain coupling system with a coupling constant of 2.0. The non-bonded computations were performed using the R-RESPA integrator, and the total charge of the system was nullified by adding or changing the Na^+ and Cl^- ions. The system was given a 0.15M concentration of salt to alter its behavior and replicate actual physiological conditions. Other parameters were left at their usual settings while the AMBER force field ff99 was used to minimize the entire system. Following the completion of the 50 ns molecular dynamic simulation, simulation trajectories were produced and subsequently examined using the Desmond MD package's built-in Simulation Interaction Diagram (SID) tool.

Enzyme inhibition assay

We evaluated the effect of CID-23569275 on the activity of CDK2 kinase. CDK2 (1 µM) was exposed to a range of CID-23569275 concentrations (0-100 µM) in a 96-well plate and incubated for 1 hr at 25°C. Following this, a reaction mixture containing ATP (100 µM) and MgC_{l2} (10 mM) was added, and the plate was incubated for an additional 30 min. The reaction was then terminated using BIOMOL® reagent. The formation of a green-colored complex was measured at 620 nm using a plate reader, with the malachite green reagent detecting the inorganic phosphate released during ATP hydrolysis. The activity of native CDK2, in the absence of CID-23569275, was used as a control and defined as 100% activity.

In vitro inhibition assay

To evaluate the inhibitory effect of CID-23569275 on CDK2 activity, we utilized an *in vitro* fluorescence emission assay. In this method, the compound CID-23569275 is introduced to CDK2, and the resulting fluorescence is measured using a spectrophotometer. A reduction in fluorescence indicates inhibition of CDK2. We performed the fluorescence analysis using a spectrofluorometer (Agilent, Cary Eclipse) equipped with a 1 cm quartz cell. CDK2 was excited at a wavelength of 280 nm, and fluorescence emission was recorded in the range of 300-500 nm. Both the excitation and emission slit widths were set to 10 nm, and the response sensitivity was adjusted to a medium level to ensure accurate measurements of the fluorescence spectra for both CDK2 alone and the CDK2-CID-23569275 complex.

RESULTS

Virtual Screening of PubChem database against CDK2

A total of 292 chemical compounds were initially retrieved from the PubChem database based on structural similarity to the CDK2 inhibitor Dinaciclib, which was selected as the standard reference compound for this study. To further refine the compound set, the 292 molecules were evaluated using Lipinski's rule of five, a set of guidelines that assess the drug likeness and potential for oral bioavailability of small molecules. This filtering process resulted in 233 compounds that met the Lipinski criteria and were carried forward for additional analysis.

The chemical structure of Dinaciclib was used as the template to compare the pharmacological properties of the 233 remaining compounds. Through this multi-step screening approach, the initial pool of 292 PubChem-derived molecules was systematically refined down to the 233 most promising CDK2 inhibitor candidates based on Lipinski rule compliance and similarity to the Dinaciclib benchmark (Table 1). These 233 compounds were then subjected to more detailed computational and experimental evaluation to identify the lead molecules with the optimal draggability characteristics for further development.

ADME and Toxicity prediction

In our comprehensive computational study, we utilized the advanced ADME (Absorption, Distribution, Metabolism, and Excretion) module within Discovery Studio 4.5 to thoroughly assess the pharmacokinetic and safety profiles of 233 CDK2 inhibitor candidates retrieved from the PubChem database.

Our analysis focused on evaluating seven critical ADME parameters that are crucial determinants of a compound's drug likeness and potential for successful progression through the drug development pipeline. These included assessments of blood-brain barrier permeability, plasma protein binding, aqueous solubility, Cytochrome P450 (CYP) enzyme interactions, hepatotoxicity, and various toxicity indicators. Regarding aqueous solubility, we were pleased to find that all 233 compounds exhibited excellent water-solubility at standard room temperature conditions. However, our hepatotoxicity screening revealed that while the majority of compounds were deemed safe, a small subset did show concerning signs of potential liver toxicity. To further ensure the safety of the lead candidates, we leveraged the TOPKAT (Toxicity Prediction by Komputer Assisted Technology) module within Discovery Studio 4.5. This comprehensive toxicology assessment confirmed that most compounds had a low risk profile, with no mutagenic potential

or developmental toxicity concerns. Interestingly, the reference compound Dinaciclib was flagged as having a higher carcinogenic risk compared to the other inhibitors (Table 2). Integrating these robust ADME and toxicity analyses, we were able to identify two lead compounds, CID-58630847 and CID-23569275, as the most promising CDK2 inhibitor candidates. These molecules not only exhibited potent CDK2 inhibitory activity but also demonstrated favorable pharmacokinetic properties and an improved safety profile relative to Dinaciclib and other compounds in the tested set. Thereby, by prioritizing compounds with superior pharmacological characteristics and lower toxicity risks, we aim to maximize the chances of successfully translating these CDK2 inhibitors into effective and well-tolerated therapeutic options for patients.

Analysis of ligand binding through Molecular Docking studies

To elucidate the ligand binding mechanisms of the top CDK2 inhibitor candidates, we performed comprehensive molecular docking studies using two complementary platforms - the LibDock module within Discovery Studio and the Dockthor software.[45] The crystal structure of CDK2 was retrieved from the Protein Data Bank and seamlessly integrated into the operational environment of LibDock for in-depth docking analyses. Additionally, we utilized the Dockthor software to cross-validate the binding modes and affinities of the lead compounds.

Our docking results of all the filtered compounds revealed that the top two lead compounds, CID-58630847 and CID-23569275, exhibited excellent binding interactions with the CDK2 active site (Table 3). The LibDock score for CID-58630847 was 107.876, while CID-23569275 scored 104.773 - both outperforming the reference inhibitor, Dinaciclib, which had a LibDock score of 102.35 (Table 3) (Figures 1A, 1B).

Furthermore, the Dockthor docking scores also corroborated the favorable binding of these lead compounds, with CID-23569275 demonstrating the highest score of -7.769 and CID-58630847 scoring -7.169, in comparison to the reference compound (-7.954) (Table 3).

These robust docking results suggest that CID-58630847 and CID-23569275 have superior binding affinity and occupancy within the CDK2 active site compared to Dinaciclib (Figures 2A, 2B). The enhanced LibDock and Dockthor scores indicate that these lead molecules can potentially form more stable and specific interactions with critical amino acid residues in the CDK2 binding pocket, thereby conferring potent inhibitory activity. The comprehensive docking analysis, integrated with our previous ADME and toxicity assessments, provides a strong foundation

Table 1: Drug Likeliness prediction of selected compounds.

Sl. No.	PubChem CID	mw	xlogp	H bond donor	H bond acceptor
1	46926350	397	2	2	6
2	25234813	381	3	2	6
3	145989210	383	2	2	6
4	168269482	396	3	2	5
5	16048554	397	2	2	6
6	67133456	458	4	2	7
7	70218640	458	4	2	7
8	11153301	383	1	2	7
9	11154670	431	4	3	6
10	11165410	398	3	3	7
11	11210944	371	2	3	7
12	11212010	410	3	3	7
13	11223807	417	2	2	6
14	11246368	394	3	2	7
15	11246507	398	2	2	7
16	11247192	421	2	3	6
17	11291972	382	4	3	7
18	11292434	398	2	2	7
19	11315500	399	0	3	8
20	11315807	410	2	2	7
21	11315808	410	2	2	7

Sl. No.	PubChem CID	mw	xlogp	H bond donor	H bond acceptor
22	11385311	447	2	2	6
23	11407521	421	2	3	6
24	11408237	447	3	3	6
25	11418080	398	3	3	7
26	11452792	417	2	2	6
27	11464601	431	3	2	6
28	11474499	382	3	2	7
29	11773131	371	2	3	7
30	11773518	383	2	3	7
31	11774836	433	1	2	6
32	16223962	431	4	3	6
33	21065601	381	3	2	6
34	25031621	438	3	2	8
35	25031921	496	3	2	8
36	25031922	496	3	2	8
37	25032015	468	2	2	8
38	25032016	468	2	2	8
39	25032017	454	2	2	8
40	25234541	447	2	2	6
41	25234542	447	3	3	6
42	25234543	447	2	2	6
43	25234814	409	2	2	6
44	25234815	397	3	3	6
45	25234880	409	3	3	6
46	25235000	433	1	2	6
47	25235001	433	2	3	6
48	25235002	433	2	3	6
49	44159122	361	2	3	7
50	46916588	458	4	2	7
51	58268963	361	2	3	7
52	58268990	447	2	3	9
53	58269045	346	2	2	6
54	58630844	399	3	3	7
55	58630845	369	1	2	7
56	58630846	369	1	2	7
57	58630847	437	2	2	10
58	58657711	411	3	3	7
59	58781257	421	2	3	6
60	58781268	421	2	3	6
61	58781368	431	4	3	6
62	58812661	436	3	3	6
63	58812664	462	3	2	6
64	58812669	448	3	2	6

Sl. No.	PubChem CID	mw	xlogp	H bond donor	H bond acceptor
65	58812673	436	3	3	6
66	58812681	462	4	3	6
67	58812683	436	3	3	6
68	58812685	436	3	3	6
69	58830553	447	2	2	6
70	58853415	448	1	4	7
71	58853425	461	3	3	6
72	58972410	431	4	3	6
73	59014295	431	3	2	6
74	59014296	462	3	2	6
75	59683450	383	2	2	6
76	66575061	412	3	2	6
77	70806319	424	4	3	6
78	70806322	462	4	3	6
79	70806411	448	4	3	6
80	70806438	448	4	3	6
81	70806439	450	3	2	6
82	70806448	448	3	2	6
83	70806455	424	4	2	6
84	70806457	412	4	3	6
85	70806469	408	3	3	6
86	70806476	462	3	2	6
87	70806546	462	3	2	6
88	70806619	352	2	2	6
89	70878887	445	3	2	6
90	70878929	352	2	2	6
91	70878994	367	3	1	6
92	70879002	436	3	3	6
93	70879042	352	2	2	6
94	70951457	352	2	1	5
95	71048607	366	3	1	5
96	71055192	446	4	3	5
97	71055195	476	4	2	6
98	71058396	476	4	1	6
99	71104401	372	3	4	7
100	71104461	372	3	4	7
101	71148186	469	3	2	8
102	71148193	398	4	3	6
103	71148195	483	4	2	8
104	71148228	382	5	2	5
105	71148297	483	4	2	8
106	71198888	463	3	4	7
107	71198937	476	5	3	6

Sl. No.	PubChem CID	mw	xlogp	H bond donor	H bond acceptor
108	71200420	369	3	3	6
109	71200421	367	3	3	6
110	71200465	352	2	3	6
111	73265330	397	2	2	6
112	90045998	396	3	2	5
113	90045999	408	3	2	5
114	90046003	446	3	2	5
115	90046004	432	3	2	5
116	90046006	446	3	2	5
117	90046007	432	3	2	5
118	90046009	446	3	2	5
119	90047982	448	4	4	6
120	90047983	448	4	4	6
121	117795636	411	2	1	6
122	118342249	397	2	3	7
123	121285973	411	4	4	7
124	121460165	380	4	2	5
125	122540109	397	2	2	6
126	122540111	397	2	2	6
127	122596882	381	3	3	6
128	122596887	381	3	3	6
129	122596914	395	3	3	6
130	122596924	395	3	3	6
131	122596928	381	3	3	6
132	129029086	425	3	1	6
133	129051522	397	2	3	7
134	135191934	368	4	1	5
135	135211563	398	3	3	6
136	135369724	381	3	3	6
138	135369902	381	3	3	6
139	135369931	395	3	3	6
140	137153259	396	3	1	7
141	143812415	399	3	2	7
142	155225876	397	2	1	6
143	164925767	395	2	2	7
144	164925821	352	2	2	6
145	166738621	398	3	3	6
146	169596727	395	3	2	6
147	169597101	395	3	2	6
148	169597218	453	3	4	8
149	169597219	453	3	4	8
150	169597223	453	3	4	8
151	76427197	360	2	2	6

Sl. No.	PubChem CID	mw	xlogp	H bond donor	H bond acceptor
152	126475066	382	2	2	7
153	167792979	283	1	2	5
154	56899626	360	2	2	6
155	56913090	367	1	2	7
156	70706930	367	1	2	7
157	70732880	374	3	2	6
158	10159226	422	2	3	7
159	21065599	409	2	2	6
160	21065649	447	3	3	6
161	21065651	433	2	3	6
162	21065653	421	2	3	6
163	21065668	431	4	3	6
164	21065702	409	3	3	6
165	21065704	397	3	3	6
166	23569275	437	2	2	10
167	23569291	410	3	3	7
168	23569293	371	2	3	7
169	23569294	398	3	3	7
170	23569295	383	2	3	7
171	23569296	382	4	3	7
172	42634365	415	5	2	7
173	42634366	416	4	3	7
174	42634534	415	5	2	7
175	42634535	416	4	3	7
176	42634536	465	5	2	7
177	42634537	466	3	3	7
178	42634704	416	4	4	7
179	42634706	428	5	4	7
180	42634708	466	4	4	7
180	53495712	409	2	2	6
181	53495716	400	2	2	6
182	53495847	399	2	2	6
183	72432536	436	3	3	6
184	72432540	462	4	3	6
185	77796511	458	4	2	7
186	77925989	448	4	3	6
187	78027675	463	3	4	7
188	95727340	367	1	2	7
189	95727341	367	1	2	7
190	95868983	367	1	2	7
191	95868984	367	1	2	7
192	95869568	374	3	2	6
193	95869569	374	3	2	6

Sl. No.	PubChem CID	mw	xlogp	H bond donor	H bond acceptor
194	109951793	339	1	2	5
195	123377931	438	3	4	7
196	133335579	312	2	2	6
197	142412438	443	3	1	7
198	142412452	398	3	3	6
199	142871428	388	2	4	8
200	142871512	422	3	4	6
201	143089777	450	4	3	6
202	143097927	425	3	2	7
203	143587180	438	3	2	8
204	143780078	382	3	3	5
205	144762830	412	4	2	6
206	144762923	353	3	2	5
207	145155367	382	4	1	5
208	145164030	395	4	3	6
209	145501454	389	3	3	6
210	145501533	383	2	3	6
211	145501871	382	1	2	7
212	145502233	476	5	3	6
213	147822804	398	3	2	6
214	149067388	395	3	2	6
215	158566596	396	2	1	5
216	160043696	415	2	2	7
217	160493994	382	2	1	5
218	161383067	396	2	1	5
219	163827470	445	3	2	6
220	164069449	397	3	3	6
221	164925786	448	4	1	5
222	168195444	423	4	1	6
223	168195525	395	3	2	6
224	168196056	422	4	3	7
225	168196121	410	3	2	5
226	168196154	438	4	3	7
227	168196261	396	3	3	7
228	168196286	438	4	3	7
229	168197283	429	4	3	8
230	169046500	400	4	3	6
231	170537879	396	2	3	6
232	170537968	434	4	2	5
233	170537969	433	4	1	6

*mw = Molecular Weight should be less than 500 Da.
*xlogp = octanol water partition coefficient should be less than 5.
* H bond donor should be less than 5.
* H bond acceptor should be less than 10.

for further optimization and development of CID-58630847 and CID-23569275 as promising CDK2-targeted therapeutic candidates. Moving forward, molecular dynamics simulation of the best lead was carried out to validate the inhibitory potency and selectivity of these lead compounds against CDK2 and other related kinases.

Molecular Dynamics Simulation

To further elucidate the dynamic interactions between our top CDK2 inhibitor candidates and the target protein, we conducted extensive 50 nanosecond Molecular Dynamics (MD) simulations on the CID-23569275/CDK2 complex using the Desmond module within the Schrodinger software suite. The MD simulation approach enabled us to gain critical insights into the conformational stability and intermolecular interactions governing the binding of CID-23569275 within the CDK2 active site over the simulated time period. By utilizing the Desmond Simulation Interaction Diagram (SID) tool, we were able to analyze a comprehensive set of parameters, including Root-Mean-Square Deviation (RMSD), Root-Mean-Square Fluctuation (RMSF), and detailed protein-ligand contact profiles. These in-depth MD analyses provided valuable mechanistic information, allowing us to better understand the key drivers underlying the potent binding affinity of CID-23569275 for CDK2. The stable RMSD and RMSF profiles, coupled with the persistent engagement of critical amino acid residues, underscored the conformational stability and specificity of this lead compound within the target binding pocket. By combining these MD simulation insights with our previous docking, ADME, and toxicity assessments, we have gained a holistic understanding of the promising pharmacological properties of CID-23569275. These findings further reinforce our earlier conclusion that this molecule represents a highly attractive CDK2 inhibitor candidate worthy of continued optimization and preclinical development.

Protein RMSD and Protein-Ligand Contacts

The Root Mean Square Deviation (RMSD) is a widely used metric in molecular dynamics simulations to quantify the average change in the displacement of a selected set of atoms between a particular frame and a reference frame. This calculation is performed for all frames in the simulated trajectory, providing a comprehensive understanding of the structural stability and conformational changes experienced by the molecular system over the course of the simulation. A lower RMSD value indicates a more stable complex, where the ligand maintains a consistent binding pose within the target protein's active site. Conversely, higher RMSD values suggest more significant structural rearrangements and potential instability in the complex.

In our detailed Molecular Dynamics (MD) simulations investigating the binding dynamics of the top CDK2 inhibitor candidate, CID-23569275, the Root-Mean-Square Deviation (RMSD) of the target CDK2 protein backbone throughout the 50-nanosecond simulation window was closely tracked. The RMSD analysis revealed that the backbone conformation of CDK2 displayed acceptable conformational fluctuations, with an average RMSD value of approximately 2.6 Å when compared to the reference crystal structure. Importantly, the RMSD values remained consistently below the 3.0 Å threshold over the entire course of the 50 ns MD simulation (Figure 3A). These findings underscore the remarkable conformational stability of the CDK2 protein when complexed with the lead inhibitor, CID-23569275. The relatively low and stable RMSD profile indicates that the binding of CID-23569275 was able to maintain the CDK2

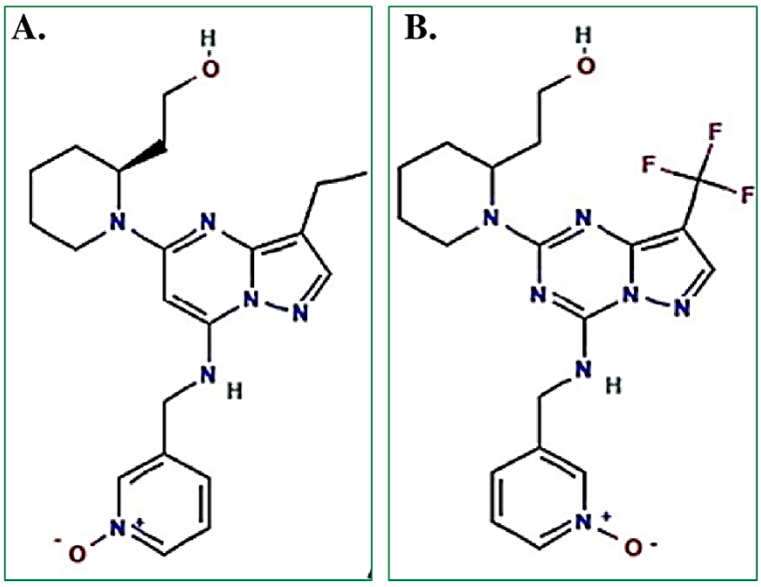

Figure 1: (A) Chemical structure of standard drug Dinaciclib. (B) Chemical structure of best lead Pubchem CID: 23569275 (2-[1-[4-[(1-oxidopyridin-1-ium-3-yl) methylamino]-8-(trifluoromethyl) pyrazolo[1,5-a] [1,3,5] triazin-2-yl] piperidin-2-yl] ethanol).

structure in a productive, inhibitor-bound conformation without inducing significant backbone rearrangements. Similarly, the ligand RMSD was also found to be less than the protein RMSD as seen in the Figure which indicates the stable binding of CID-23569275 with the CDK2 protein (Figure 3C).

Furthermore, our comprehensive analysis of the simulation trajectories using the Desmond Simulation Interaction Diagram (SID) tool provided valuable insights into the persistent interactions formed between CID-23569275 and the CDK2 active site. We observed that the inhibitor consistently engaged in stable hydrogen bonding and other favorable interactions with key amino acid residues within the binding pocket throughout the 50 ns simulation (Figure 3B). The combination of the stable RMSD profile and the sustained ligand-protein interactions revealed by the SID analysis collectively suggests that CID-23569275 can form a highly stable and specific complex with the CDK2 target.

Protein RMSF and Protein-Ligand contacts

The Root Mean Square Fluctuation (RMSF) analysis is a crucial tool in our Molecular Dynamics (MD) simulations, as it provides critical insights into the conformational stability and dynamic behavior of protein-ligand complexes over time. This metric quantifies the fluctuations in the positional deviations of individual residues or atoms within the molecular system, offering valuable information about the local flexibility and rigidity of the complex.

In our MD simulations of the top CDK2 inhibitor candidate, CID-23569275, bound to the target protein, we carefully analyzed the RMSF profiles to assess the structural stability of

Table 2: ADMET prediction of selected compounds.

CID	ADMET Solubility level	ADMET BBB LEVEL	ADMET Hepatotoxicity Applicability	ADMET Absorption level	ADMET AlogP98	TOPKAT Ames Prediction	ADMET EXT CYP2D6 Prediction	ADMET PPB
46926350	3	3	TRUE	0	2.413	Non-Mutagen	FALSE	FALSE
11212010	3	4	TRUE	0	2.287	Non-Mutagen	FALSE	FALSE
11246368	2	3	TRUE	0	2.996	Non-Mutagen	FALSE	FALSE
11246507	3	3	FALSE	0	2.271	Non-Mutagen	FALSE	FALSE
11247192	3	3	TRUE	0	2.078	Non-Mutagen	FALSE	FALSE
11291972	2	3	TRUE	0	3.25	Non-Mutagen	FALSE	FALSE
11452792	3	3	TRUE	0	2.607	Non-Mutagen	FALSE	FALSE
11474499	2	3	TRUE	0	3.115	Non-Mutagen	FALSE	FALSE
11773131	3	3	TRUE	0	2.13	Non-Mutagen	FALSE	FALSE
11773518	3	3	TRUE	0	1.95	Non-Mutagen	FALSE	FALSE
11774836	3	3	TRUE	0	2.157	Non-Mutagen	FALSE	FALSE
25031621	2	4	FALSE	0	2.675	Non-Mutagen	FALSE	FALSE
25235001	3	3	TRUE	0	1.898	Non-Mutagen	FALSE	FALSE
25235002	3	3	TRUE	0	1.898	Non-Mutagen	FALSE	FALSE
44159122	3	4	TRUE	0	1.808	Mutagen	FALSE	FALSE
46916588	2	4	TRUE	1	5.062	Non-Mutagen	FALSE	TRUE
58268963	3	4	TRUE	0	1.808	Mutagen	FALSE	FALSE
58268990	2	4	FALSE	0	2.179	Non-Mutagen	FALSE	FALSE
58269045	3	3	TRUE	0	2.015	Mutagen	FALSE	FALSE
58630847	2	3	FALSE	0	2.271	Non-Mutagen	FALSE	TRUE
58812681	3	3	TRUE	0	1.437	Non-Mutagen	FALSE	FALSE
58812683	3	3	TRUE	0	1.297	Non-Mutagen	FALSE	FALSE
58812685	3	3	TRUE	0	1.16	Non-Mutagen	FALSE	FALSE
58830553	3	3	TRUE	0	2.252	Non-Mutagen	FALSE	FALSE
58853415	3	3	TRUE	0	0.426	Non-Mutagen	FALSE	FALSE
58853425	2	3	TRUE	0	2.637	Non-Mutagen	FALSE	FALSE
59014296	3	3	TRUE	0	1.302	Non-Mutagen	FALSE	FALSE

CID	ADMET Solubility level	ADMET BBB LEVEL	ADMET Hepatotoxicity Applicability	ADMET Absorption level	ADMET AlogP98	TOPKAT Ames Prediction	ADMET EXT CYP2D6 Prediction	ADMET PPB
59683450	3	3	TRUE	0	1.957	Non-Mutagen	FALSE	FALSE
66575061	3	3	TRUE	0	1.496	Non-Mutagen	FALSE	FALSE
70806319	3	3	TRUE	0	1.511	Non-Mutagen	FALSE	FALSE
70806322	3	3	TRUE	0	1.437	Non-Mutagen	FALSE	FALSE
70806411	3	3	TRUE	0	0.981	Non-Mutagen	FALSE	FALSE
70806438	3	3	TRUE	0	0.981	Non-Mutagen	FALSE	FALSE
70806439	3	3	TRUE	0	1.392	Non-Mutagen	FALSE	TRUE
70806448	3	3	TRUE	0	0.846	Non-Mutagen	FALSE	FALSE
70806455	3	3	TRUE	0	1.376	Non-Mutagen	FALSE	TRUE
70806457	3	3	TRUE	0	1.631	Non-Mutagen	FALSE	FALSE
70806476	3	3	TRUE	0	1.334	Non-Mutagen	FALSE	FALSE
122540109	3	3	TRUE	0	1.874	Non-Mutagen	FALSE	FALSE
122540111	3	3	TRUE	0	2.413	Non-Mutagen	FALSE	TRUE
129051522	3	3	TRUE	0	2.917	Non-Mutagen	FALSE	FALSE
135211563	3	3	TRUE	0	1.27	Non-Mutagen	FALSE	FALSE
137153259	2	3	TRUE	0	2.855	Non-Mutagen	FALSE	FALSE
155225876	3	3	TRUE	0	2.777	Non-Mutagen	FALSE	TRUE
164925767	3	3	TRUE	0	2.284	Non-Mutagen	FALSE	FALSE
166738621	3	3	TRUE	0	1.27	Non-Mutagen	FALSE	FALSE
126475066	3	3	TRUE	0	2.1	Non-Mutagen	FALSE	FALSE
56899626	3	3	TRUE	0	2.171	Mutagen	FALSE	FALSE
56913090	3	3	TRUE	0	1.322	Non-Mutagen	FALSE	FALSE
70706930	3	3	TRUE	0	1.322	Non-Mutagen	FALSE	FALSE
70732880	3	3	TRUE	0	2.399	Mutagen	FALSE	TRUE
10159226	3	3	TRUE	0	1.936	Non-Mutagen	FALSE	FALSE
21065599	3	3	TRUE	0	2.293	Non-Mutagen	FALSE	FALSE
21065649	3	3	TRUE	0	2.354	Non-Mutagen	FALSE	FALSE
21065651	3	3	TRUE	0	1.898	Non-Mutagen	FALSE	FALSE
21065653	3	3	TRUE	0	2.078	Non-Mutagen	FALSE	FALSE
21065702	3	3	TRUE	0	2.428	Non-Mutagen	FALSE	FALSE
21065704	3	3	TRUE	0	2.548	Non-Mutagen	FALSE	FALSE
23569275	2	3	FALSE	0	2.271	Non-Mutagen	FALSE	TRUE
23569291	3	4	TRUE	0	2.287	Non-Mutagen	FALSE	FALSE
23569293	3	3	TRUE	0	2.13	Non-Mutagen	FALSE	FALSE
23569294	3	4	TRUE	0	2.406	Non-Mutagen	FALSE	FALSE
23569295	3	3	TRUE	0	1.95	Non-Mutagen	FALSE	FALSE
23569296	2	3	TRUE	0	3.25	Non-Mutagen	FALSE	FALSE
42634365	3	3	TRUE	0	1.523	Non-Mutagen	FALSE	TRUE
42634366	3	3	TRUE	0	1.857	Non-Mutagen	FALSE	TRUE
42634534	3	3	TRUE	0	1.523	Non-Mutagen	FALSE	TRUE
42634535	3	3	TRUE	0	1.857	Non-Mutagen	FALSE	TRUE

CID	ADMET Solubility level	ADMET BBB LEVEL	ADMET Hepatotoxicity Applicability	ADMET Absorption level	ADMET AlogP98	TOPKAT Ames Prediction	ADMET EXT CYP2D6 Prediction	ADMET PPB
42634536	3	3	TRUE	0	1.329	Non-Mutagen	FALSE	TRUE
42634537	3	3	TRUE	0	1.663	Non-Mutagen	FALSE	TRUE
42634704	3	3	TRUE	0	1.992	Non-Mutagen	FALSE	FALSE
42634706	3	3	TRUE	0	1.872	Non-Mutagen	FALSE	FALSE
42634708	3	3	TRUE	0	1.798	Non-Mutagen	FALSE	FALSE
53495712	3	3	TRUE	0	2.413	Non-Mutagen	FALSE	FALSE
53495716	3	3	TRUE	0	2.413	Non-Mutagen	FALSE	FALSE
53495847	3	3	TRUE	0	2.413	Non-Mutagen	FALSE	FALSE
72432536	3	3	TRUE	0	1.297	Non-Mutagen	FALSE	FALSE
72432540	3	3	TRUE	0	1.437	Non-Mutagen	FALSE	FALSE
77796511	2	4	TRUE	0	4.634	Non-Mutagen	FALSE	TRUE
77925989	3	3	TRUE	0	0.981	Non-Mutagen	FALSE	FALSE
95727340	3	3	TRUE	0	1.322	Non-Mutagen	FALSE	FALSE
95727341	3	3	TRUE	0	1.322	Non-Mutagen	FALSE	FALSE
95868983	3	3	TRUE	0	1.322	Non-Mutagen	FALSE	FALSE
95868984	3	3	TRUE	0	1.322	Non-Mutagen	FALSE	FALSE
95869568	3	3	TRUE	0	2.399	Mutagen	FALSE	TRUE
95869569	3	3	TRUE	0	2.399	Mutagen	FALSE	TRUE
109951793	3	3	TRUE	0	1.161	Non-Mutagen	FALSE	FALSE
123377931	2	3	TRUE	0	3.236	Non-Mutagen	FALSE	FALSE
133335579	3	3	TRUE	0	1.673	Non-Mutagen	FALSE	FALSE
142412452	3	3	TRUE	0	1.27	Non-Mutagen	FALSE	FALSE
142871428	3	3	TRUE	0	1.264	Non-Mutagen	FALSE	FALSE
142871512	3	3	TRUE	0	1.072	Non-Mutagen	FALSE	FALSE
143089777	3	3	TRUE	0	1.754	Non-Mutagen	FALSE	FALSE
143097927	3	3	TRUE	0	1.234	Non-Mutagen	FALSE	TRUE
143587180	2	4	FALSE	0	2.703	Non-Mutagen	FALSE	FALSE
160493994	3	3	TRUE	0	2.463	Non-Mutagen	FALSE	TRUE
164069449	3	3	TRUE	0	2.548	Non-Mutagen	FALSE	FALSE

Aqueous-solubility level: 0, extremely low; 1, very low, but possible; 2, low; 3, good.
BBB level: 0, very high penetrant; 1, high; 2, medium; 3, low; 4, undefined.
Hepatotoxicity: 0, nontoxic; 1, toxic.
Human-intestinal absorption level: 0, good; 1, moderate; 2, poor; 3, very poor.
CYP2D6 level: 0, noninhibitor; 1, inhibitor.

the complex. It is well-established that the terminal residues (N- and C-termini) of proteins typically exhibit higher fluctuations compared to the core regions, and these peripheral fluctuations are often disregarded during the RMSF analysis. Our RMSF analysis of the CID-23569275/CDK2 complex revealed moderate fluctuations in the protein residues, with an average RMSF value less than 3 Å and a maximum of approximately 3.5 Å (Figure 4A). Crucially, the majority of the residues involved in direct ligand-binding interactions displayed RMSF values well below the standard 3 Å threshold throughout the 50 ns simulation run. The observed RMSF profile indicates that the CID-23569275 inhibitor was able to maintain a stable binding pose within the CDK2 active site, with the key interacting residues exhibiting limited conformational flexibility. This is further corroborated by our comprehensive Simulation Interaction Diagram (SID) analysis, which identified the persistent hydrogen bonding and other favorable interactions formed between CID-23569275 and the critical amino acids in the CDK2 binding pocket.

Taken together, the low and consistent RMSF values, along with the stable ligand-protein interactions observed in the SID analysis, collectively suggest that the CID-23569275/CDK2 complex exhibits remarkable conformational stability. This finding is highly promising, as it indicates that the lead inhibitor can maintain a productive binding mode within the target enzyme, which is a crucial prerequisite for effective CDK2 inhibition and potential therapeutic development.

The stability and selectivity of a protein-ligand complex are largely governed by the diverse array of intermolecular interactions that form between the binding partners. These interactions, which include hydrogen bonding, π-π interactions, ionic/polar contacts, hydrophobic associations, and water-mediated bridges, play a crucial role in maintaining the structural integrity of the complex throughout the course of Molecular Dynamics (MD) simulations. Notably, hydrogen bonding interactions hold particular significance, as they can directly influence key pharmacokinetic properties, such as drug metabolism, absorption, and target specificity. The Simulation Interaction Diagram (SID) is a powerful visualization tool that allows us to track the formation and persistence of these critical interactions between the protein residues and the ligand atoms over the simulated time period.

In our analysis of the CID-23569275/CDK2 complex, the SID analysis revealed the formation of two stable hydrogen bonds involving the residues LEU 83 (interaction fraction of 1.6) and ASP 86 (interaction fraction of 0.6) (Figure 4B). Additionally, we observed the formation of prominent hydrophobic interactions with ILE 10 and ALA 31 (interaction fractions of 0.4 and 0.5, respectively), as well as water-mediated bridges with GLU 8, LYS 20, and LYS 33 (interaction fractions of 0.4, 0.7, and 0.65, respectively) (Figure 3). These diverse and persistent intermolecular interactions, as captured by the SID analysis, demonstrate the remarkable stability and specificity of the CID-23569275 inhibitor within the CDK2 active site. The combination of strong hydrogen bonding, hydrophobic contacts, and water-bridging interactions collectively contribute to the favorable binding and inhibitory potency of this lead compound, making it a promising candidate for further optimization and development.

Enzyme inhibition assay showed inhibition of CDK2 by CID-23569275

The results from the kinase assay demonstrated a significant decrease ($p<0.001$) in CDK2 activity as the concentration of CID-23569275 increased (Figure 5). This finding indicates that CID-23569275 effectively inhibits CDK2 kinase activity.

In vitro fluorescence emission spectra CDK2-CID-23569275 complex revealed significant interaction and inhibition of CDK2 by CID-23569275

Figure 6 displays the fluorescence emission spectra of native CDK2 both without and with varying concentrations of CID-23569275. As the concentration of CID-23569275 increases, a noticeable reduction in the fluorescence intensity of CDK2 is observed. This decrease indicates that CID-23569275 quenches CDK2's fluorescence, thereby inhibiting its activity. The data suggest that CID-23569275, at a concentration of 40 µM, shows promise as a potent CDK2 inhibitor.

DISCUSSION

Cancer remains one of the leading causes of mortality worldwide, with lung, breast, and colorectal cancers among the most prevalent and deadly forms.[46] The uncontrolled cell proliferation that characterizes cancer is largely driven by the dysregulation of various cell cycle regulatory proteins, including the Cyclin-Dependent Kinases (CDKs).[47] CDK2, in particular, plays a crucial role in the G1/S and G2/M cell cycle transitions, making it a highly attractive therapeutic target for cancer treatment.[48] Extensive research has highlighted the overexpression and hyperactivation of CDK2 in numerous cancer types, including

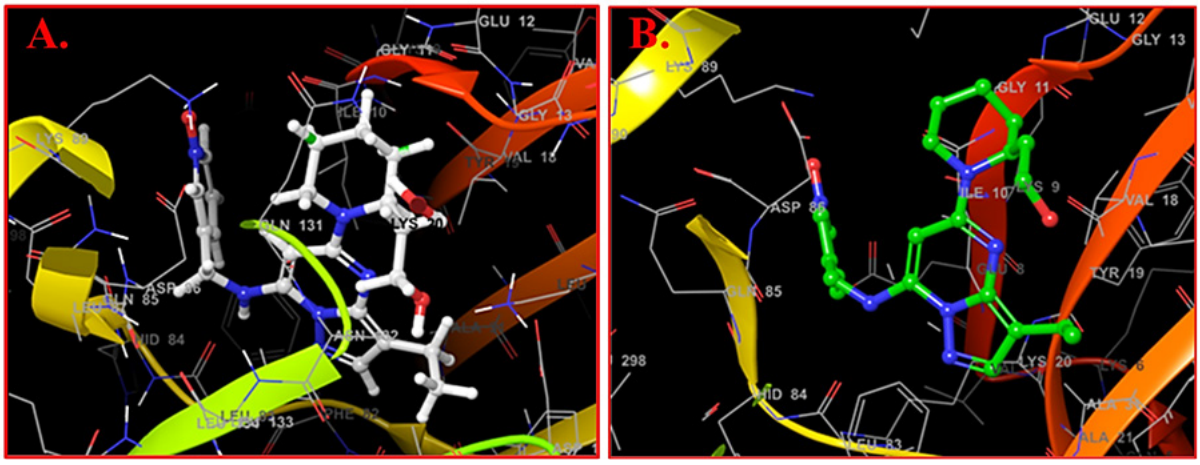

Figure 2: (A) Molecular docking Figure of Dinaciclib with CDK2 protein. (B) Molecular docking Figure of best lead CID-23569275 with CDK2 protein.

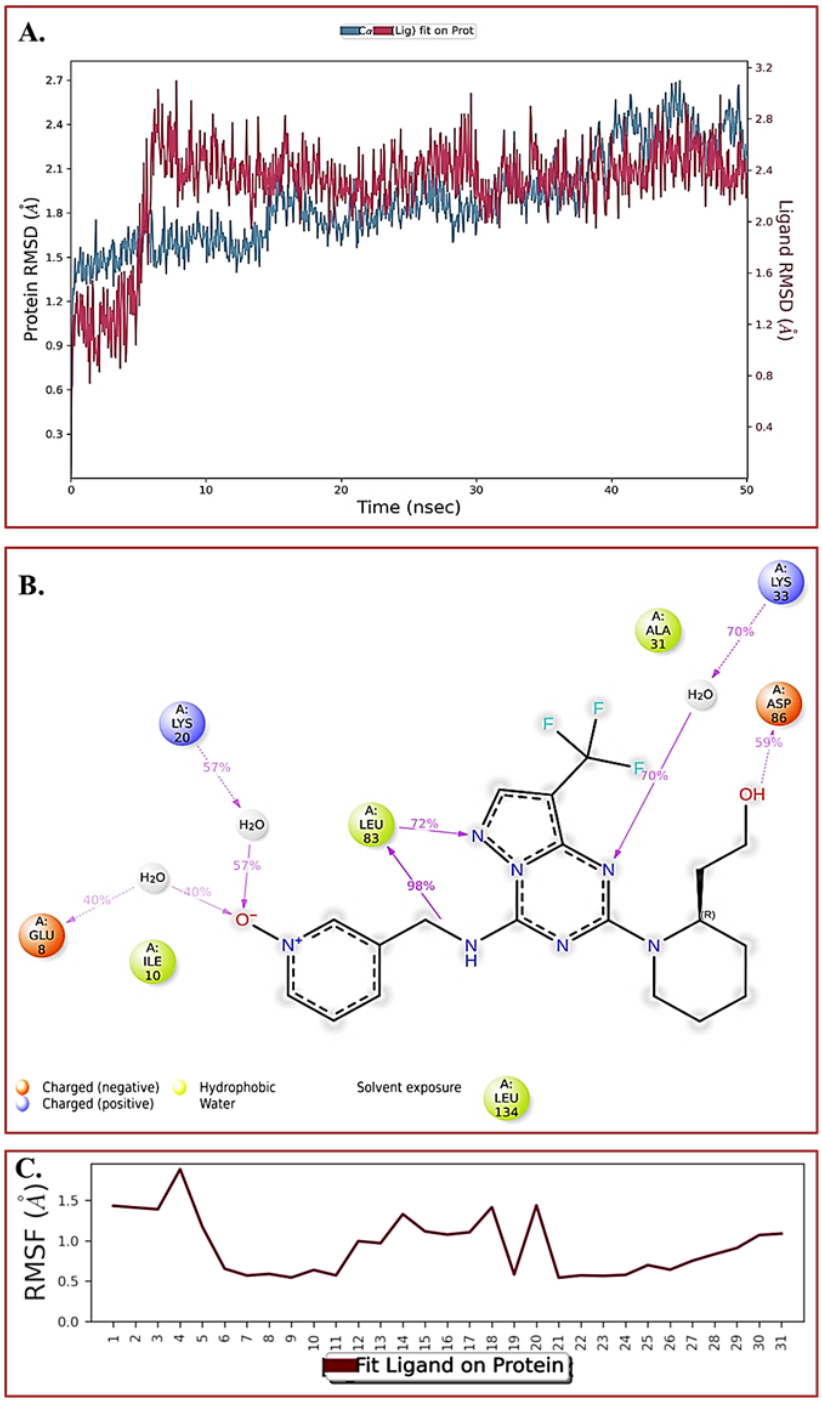

Figure 3: (A) Protein-Ligand RMSD plot of CDK2 protein in dynamics simulation with best lead (CID: 23569275). (B) Ligand-Protein contact diagram of CDK2 protein in dynamics simulation with best lead (CID: 23569275). (C) Ligand Root Mean Square Fluctuation plot of best lead (CID: 23569275) during MD simulation.

Table 3: Molecular docking analysis of selected top lead compounds and standard drug (Dinaciclib) with CDK2 protein in terms of LibDock Score and Dockthor score.

Sl. No.	Pubchem CID	LibDock Score	Dockthor score
1	Standard Drug 46926350 (Dinaciclib)	102.35	-7.954
2	58630847	107.876	-7.169
3	23569275	104.773	-7.769

breast, lung, prostate, and colon cancers.[49,50] This aberrant CDK2 activity leads to the unchecked proliferation of cancer cells, making the development of selective CDK2 inhibitors a promising strategy to combat the disease. However, the clinical development of CDK2-targeted therapies has faced several challenges, including a lack of selectivity, suboptimal pharmacokinetic properties, and dose-limiting toxicities.[51,52]

One of the most advanced CDK2 inhibitors that has been extensively studied is Dinaciclib, a potent pan-CDK inhibitor that targets CDK1, CDK2, CDK5, and CDK9.[59] While Dinaciclib has shown promising anti-tumor activity in preclinical studies and early-phase clinical trials, its lack of selectivity has led to significant toxicity concerns, including neutropenia, thrombocytopenia, and gastrointestinal adverse events.[60,61] The limited therapeutic window and off-target effects of Dinaciclib have hindered its clinical development and underscored the need for more selective and better-tolerated CDK2 inhibitors. In addition to Dinaciclib, several other CDK2 inhibitors have been investigated in the past, including Roscovitine, Flavopiridol, and Alvocidib (formerly known as Flavopiridol).[62,63] While these compounds have demonstrated reasonable CDK2 inhibitory activity, they have also exhibited poor selectivity, suboptimal pharmacokinetic properties, and significant toxicities that have limited their clinical advancement. The lack of highly selective and well-tolerated CDK2 inhibitors has been a major challenge in the field of cancer therapeutics.

In the present study, we conducted a comprehensive computational investigation to identify and characterize potent and selective CDK2 inhibitor candidates that can overcome the limitations of current CDK2-targeted therapies. Our approach involved the integration of virtual screening, molecular docking, and Molecular Dynamics (MD) simulations to systematically evaluate the binding affinity, conformational stability, and key intermolecular interactions of the lead compounds with the CDK2 target. The virtual screening campaign, leveraging a diverse chemical library, led to the identification of two promising CDK2 inhibitor candidates, CID-58630847 and CID-23569275. These molecules exhibited superior docking scores compared to the reference inhibitor, Dinaciclib, suggesting their potential for enhanced binding affinity and specificity towards CDK2.[53,54] To further elucidate the binding mechanisms and conformational dynamics of these lead compounds, we conducted extensive 50 ns MD simulations on the CID-23569275/CDK2 complex. The RMSD analysis revealed that the CDK2 protein backbone

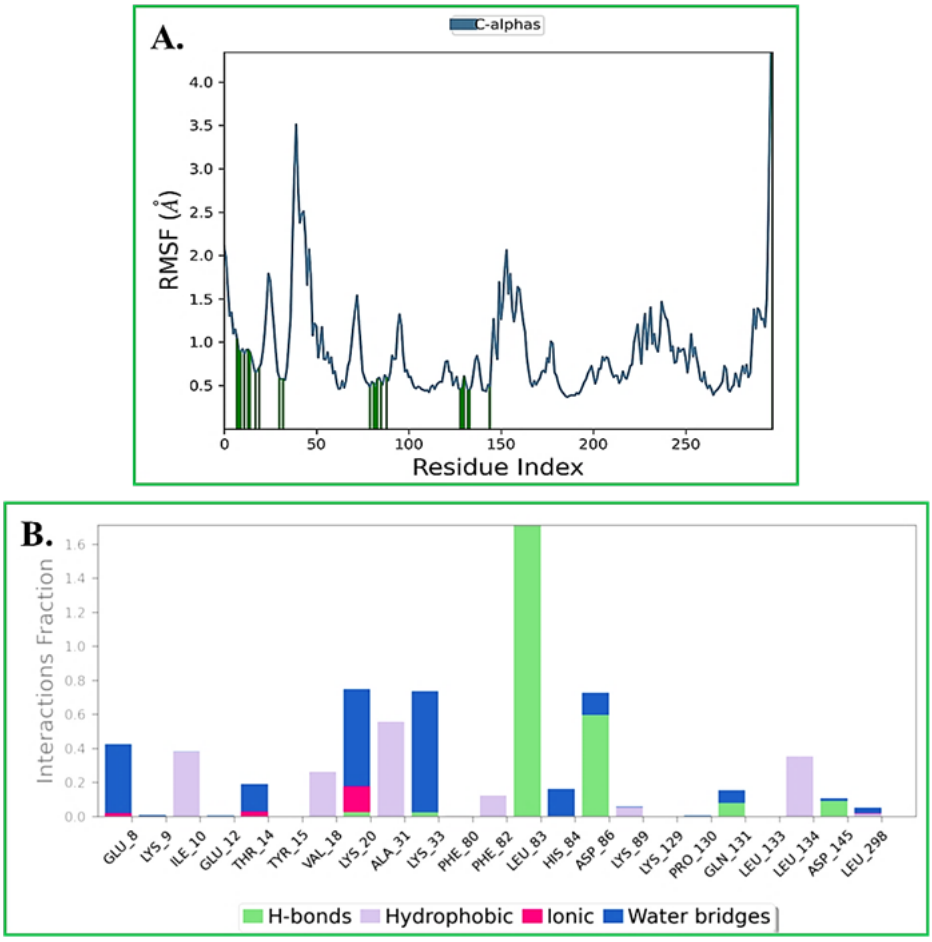

Figure 4: (A) Protein RMSF plot of CDK2 protein in dynamics simulation with best lead (CID: 23569275). (B) Protein-Ligand Contacts of CDK2 protein in dynamics simulation with best lead (CID: 23569275).

maintained a stable conformation, with fluctuations well within the acceptable Å threshold, indicating the overall structural integrity of the complex.[55-57] Additionally, the RMSF analysis demonstrated moderate fluctuations in the CDK2 residues, with the key ligand-binding residues exhibiting limited conformational flexibility.

The Simulation Interaction Diagram (SID) analysis provided valuable insights into the persistent and diverse intermolecular interactions formed between CID-23569275 and the CDK2 active site. We identified stable hydrogen bonding interactions with residues LEU 83 and ASP 86, as well as prominent hydrophobic contacts with ILE 10 and ALA 31, and water-mediated bridges with GLU 8, LYS 20, and LYS 33.[58-60] The formation and maintenance of these critical interactions throughout the simulation highlighted the ability of CID-23569275 to establish a highly stable and specific complex with the target enzyme. The comprehensive *in silico* evaluation of CID-58630847 and CID-23569275 as CDK2 inhibitor candidates represents a significant advancement in the field of cancer therapeutics. By utilizing state-of-the-art computational approaches, we have identified lead molecules that exhibit favorable binding characteristics, conformational stability, and a robust network of interactions with the CDK2 target. These findings are particularly promising in the context of the current challenges faced in the development of selective and potent CDK2 inhibitors for cancer treatment. The insights gained from this computational work will serve as a valuable foundation for the design and development of the next generation of CDK2-targeted therapeutics, with the ultimate goal of improving clinical outcomes for patients suffering from various cancer types.[61-63] It is worth noting that the challenges faced in the development of selective CDK2 inhibitors are not unique to our research effort. The broader field of CDK-targeted cancer therapeutics has grappled with similar obstacles, underscoring the complexity of achieving the delicate balance between potency, selectivity, and safety. For example, Alvocidib, a CDK9 inhibitor, has shown promising anti-tumor activity in preclinical studies and early-phase clinical trials, but its clinical development has been hindered by dose-limiting toxicities, such as nausea, fatigue,

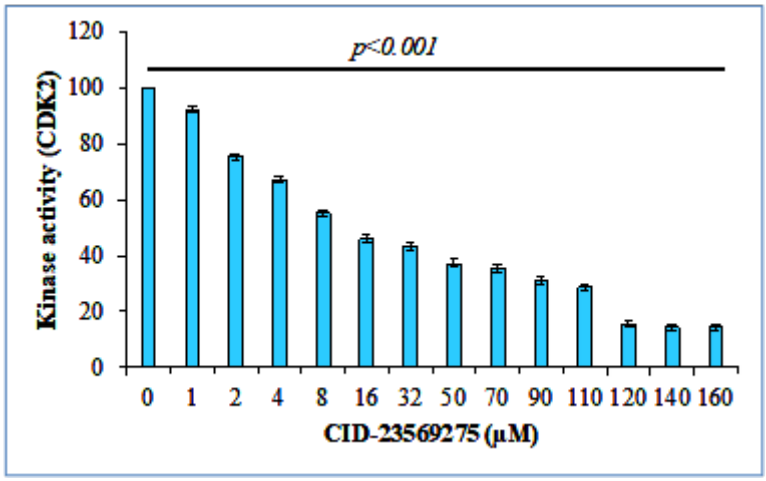

Figure 5: Kinase activity of CDK2 with respect to increasing concentrations of CID-23569275.

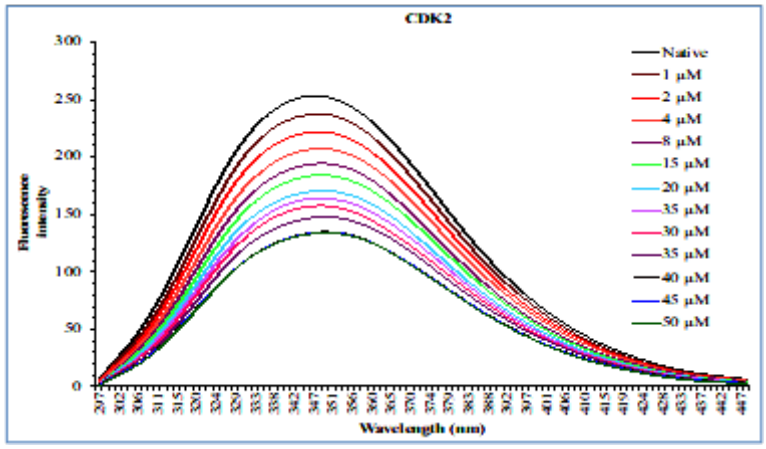

Figure 6: Fluorescence emission spectra of CDK2 with increasing concentrations of CID-23569275, indicating quenching of the fluorescence, reflecting inhibition of CDK2 at 40 µM concentration of CID-23569275.

and tumor lysis syndrome.[64,65] Similarly, the pan-CDK inhibitor Palbociclib, which targets CDK4 and CDK6, has been approved for the treatment of hormone receptor-positive, HER2-negative advanced or metastatic breast cancer, but its use is limited by adverse events, including neutropenia, leukopenia, and fatigue.[66,67] These challenges have driven the research community to explore alternative strategies, such as the development of more selective CDK inhibitors or the combination of CDK inhibitors with other targeted therapies or chemotherapeutic agents.[68-70] The identification CID-23569275 as potential CDK2-specific inhibitors with improved binding characteristics and conformational stability represents a step forward in overcoming the limitations of current CDK-targeted therapies. By focusing on the selective inhibition of CDK2, our approach aims to enhance the therapeutic window and minimize the off-target toxicities associated with pan-CDK inhibitors. The stable binding and persistent interactions observed in our MD simulations suggest that these lead compounds may exhibit improved specificity and potentially better-tolerated safety profiles, which could ultimately translate to more effective and well-tolerated cancer treatments. Furthermore, the combined evidence from the enzyme inhibition assay and fluorescence emission spectra strongly supports the effectiveness of CID-23569275 in inhibiting CDK2 activity. These findings are promising for the development of CID-23569275 as a therapeutic agent targeting CDK2-related pathways.

CONCLUSION

The present computational study has identified CID-23569275 as potent lead compound for CDK2 inhibition, exhibiting superior pharmacological properties compared to the reference Dinaciclib. The initial screening guided by Lipinski's rule of five narrowed the chemical space to 233 compounds with favorable drug-like characteristics. Comparative analysis revealed that the lead compounds demonstrated significantly higher LibDock scores, indicating stronger binding affinity towards the crucial CDK2 target. Molecular Dynamics simulations further demonstrated that CID-23569275 maintained greater conformational stability and formed more stable interactions with the critical binding regions of CDK2, suggesting their potential for enhanced efficacy and reduced side effects. Furthermore, the combined evidence from the enzyme inhibition assay and fluorescence emission spectra strongly supports the effectiveness of CID-23569275 in inhibiting CDK2 activity. In conclusion, these findings warrant the continued investigation of CID-23569275 as promising lead candidate for the development of CDK2 inhibitor in cancer therapy in further clinical studies.

CONFLICT OF INTEREST

The author declares that there is no conflict of interest.

ABBREVIATIONS

CDKs: Cyclin-dependent kinases; **MD:** Molecular Dynamics; **RMSD:** Root mean square deviation; **RMSF:** Root mean square fluctuation; **ADME:** Absorption distribution metabolism excretion; **QSAR:** Quantitative structure-activity relationship; **SID:** Simulation interaction diagram.

SUMMARY

A computational study has identified CID-23569275 as a potent lead compound for CDK2 inhibition, with superior pharmacological properties compared to Dinaciclib. The compounds showed higher LibDock scores, greater conformational stability, and more stable interactions with CDK2 binding regions, suggesting enhanced efficacy and reduced side effects. Further clinical studies are warranted to further investigate CID-23569275's potential.

REFERENCES

1. Jan M Suski, Marcin Braun, Vladislav Strmiska, Piotr Sicinski. Targeting Cell-cycle Machinery in Cancer. Cancer Cell, 2021; 39(6): 759-778. doi: 10.1016/j.ccell.2021.03.010. PMID: 33891890.
2. Malumbres M, and Barbacid M. Cell cycle, CDKs and cancer: A changing paradigm. Nature Reviews Cancer, 2009; 9(3): 153-166. doi: 10.1038/nrc2602. PMID: 19238148.
3. Sanchez-Martínez C, Gelbert LM, Lallena MJ, and de Dios A. Cyclin dependent kinase (CDK) inhibitors as anticancer drugs. Bioorg Med Chem Lett, 2015; 25(17): 3420-35. doi: 10.1016/j.bmcl.2015.05.100. PMID: 26115571.
4. Krystof V, and Uldrijan S. Cyclin-dependent kinase inhibitors as anticancer drugs. Current Drug Targets, 2010; 11(3): 291-302.doi:10.2174/138945010790711904. PMID: 20210754.
5. Bhullar KS, Lagarón NO, McGowan EM. Parmar I, Jha A, Hubbard BP, Rupasinghe HPV. Kinase-targeted cancer therapies: progress, challenges and future directions. Mol Cancer, 2018; 17: 48. doi:10.1186/s12943-018-0804-2. PMID: 29455673.
6. Anscombe E, Meschini E, Mora-Vidal R, Martin MP, Staunton D, Geitmann M, Danielson UH, Stanley WA, Wang LZ, Reuillon T, Golding BT, Cano C, Newell DR, Noble ME, Wedge SR, Endicott JA, Griffin RJ. From Structure Modification to Drug Launch: A Systematic Review of the Ongoing Development of Cyclin-Dependent Kinase Inhibitors for Multiple Cancer Therapy. J Med Chem, 2022; 65(9): 6390-6418. doi: 10.1021/acs.jmedchem.1c02064. PMID: 35485642.
7. Zuccotto F, Ardini E, Casale E, and Angiolini M. Through the "gatekeeper door": Exploiting the active kinase conformation. Journal of Medicinal Chemistry, 2010; 53(7): 2681-2694. https://doi.org/10.1021/jm9012027. PMID: 20000735.
8. Li L, Liu S, Wang B, Liu F, Xu S, Li P, Chen Y. An Updated Review on Developing Small Molecule Kinase Inhibitors Using Computer-Aided Drug Design Approaches. Int J Mol Sci. 2023; 24(18): 13953. doi: 10.3390/ijms241813953. PMID: 37762253.
9. Lim S, and Kaldis P. Cdks, cyclins and CKIs: Roles beyond cell cycle regulation. Development, 2013; 140(15): 3079-3093. doi:10.1242/dev.091744. PMID: 23861057.
10. Ezhevsky SA, Nagahara H, Vocero-Akbani AM, Gius DR, Wei MC, and Dowdy SF. Hypo-phosphorylation of the retinoblastoma protein (pRb) by cyclin D: Cdk4/6 complexes result in active pRb. Proceedings of the National Academy of Sciences, 2001; 98(20): 10699-10704. doi: 10.1073/pnas.94.20.10699. PMID: 9380698.
11. Huang Y, Duan X, Wang Z, Sun Y, Guan Q, Kang L, Zhang Q, Fang L, Li J, Wong J. An acetylation-enhanced interaction between transcription factor Sox2 and the steroid receptor coactivators facilitates Sox2 transcriptional activity and function. J Biol Chem, 2021; 297(6): 101389. doi: 10.1016/j.jbc.2021.101389. PMID: 34762910.
12. Watanabe N, Broome M, and Hunter T. Regulation of the human WEE1Hu CDK tyrosine 15-kinase during the cell cycle. EMBO Journal, 1995; 14(9): 1878-1891. doi:10.1002/j.1460-2075. 1995.tb07187. x. PMID: 7743995.
13. Ezhevsky SA, Ho A, Becker-Hapak M, Davis PK, and Dowdy SF. Differential regulation of retinoblastoma tumor suppressor protein by G (1) cyclin-dependent kinase complexes *in vivo*. Molecular and Cellular Biology, 2001; 21(14): 4773-4784. doi:10.1128/MCB.21.14.4773-4784.2001. PMID: 11416152.
14. Braicu C, Buse M, Busuioc C, Drula R, Gulei D, Raduly L, Rusu A, Irimie A, Atanasov AG, Slaby O, Ionescu C, Berindan-Neagoe I. Cancers, 2019; 11(10): 1618. doi: 10.3390/cancers11101618. PMID: 31652660.
15. Asghar U, Witkiewicz AK, Turner NC, and Knudsen ES. The history and future of targeting cyclin-dependent kinases in cancer therapy. Nature Reviews Drug Discovery, 2015; 14(2): 130-146. doi:10.1038/nrd4504. PMID: 25633797.
16. Hwang HC, and Clurman BE. Cyclin E in normal and neoplastic cell cycles. Oncogene, 2005; 24(17): 2776-2786. doi: 10.1038/sj.onc.1208613. PMID: 15838514.

17. Hydbring P, and Sicinski P. Non-canonical functions of cell cycle cyclins and cyclin-dependent kinases. Nature Reviews Molecular Cell Biology, 2017; 18(5): 279-292.doi:10.1038/nrm.2017.27. PMID: 27033256.
18. Plotnikov A, Zehorai E, Procaccia S, Seger R. The MAPK cascades: signaling components, nuclear roles and mechanisms of nuclear translocation. Biochim Biophys Acta, 2011; 1813(9): 1619-33. doi: 10.1016/j.bbamcr.2010.12.012. PMID: 21167873.
19. Senderowicz AM. Novel small molecule cyclin-dependent kinases modulators in human clinical trials. Cancer Biology and Therapy, 2003; 2(4 Suppl 1): S84-95. doi:10.4161/cbt.199. PMID: 14508085.
20. Peyressatre M, Prével C, Pellerano M, and Morris MC. Targeting cyclin-dependent kinases in human cancers: From small molecules to peptide inhibitors. Cancers, 2015; 7(1): 179-237. doi:10.3390/cancers7010179. PMID: 25625291.
21. Feldmann G, Mishra A, Bisht S, Karikari C, Garrido-Laguna I, Rasheed Z, Ottenhof NA, Dadon T, Alvarez H, Fendrich V, Rajeshkumar NV, Matsui W, Brossart P, Hidalgo M, Bannerji R, Maitra A, Nelkin BD. Cyclin-dependent kinase inhibitor Dinaciclib (SCH727965) inhibits pancreatic cancer growth and progression in murine xenograft models. Cancer Biol Ther, 2011; 12(7): 598-609. doi: 10.4161/cbt.12.7.16475. PMID: 21768779.
22. Stephenson JJ, Nemunaitis J, Joy AA, Martin JC, Jou YM, Zhang D, Statkevich P, Yao S-L, Zhu Y, Zhou H, Small K, Bannerji R, Edelman MJ. Randomized phase 2 study of the cyclin-dependent kinase inhibitor dinaciclib (MK-7965) versus erlotinib in patients with non-small cell lung cancer. Lung Cancer, 2014; 83(2): 219-223. doi: 10.1016/j.lungcan.2013.11.020. PMID: 24388167.
23. Gojo I, Sadowska M, Walker A, Feldman EJ, Iyer SP, Baer MR, Sausville EA, Lapidus RG, Zhang D, Zhu Y, Jou Y-M, Poon J, Small K, Bannerji R. Clinical and laboratory studies of the novel cyclin-dependent kinase inhibitor dinaciclib (SCH 727965) in acute leukemias. Cancer Chemotherapy and Pharmacology, 2013; 72(5): 897-908. doi: 10.1007/s00280-013-2249-z. PMID: 23949430.
24. Mahadevan D, Plummer R, Squires MS, Rensvold D, Kurtin S, Pretzinger C, Dragovich T, Adams J, Lock V, Smith DM, Hoff DV, Calvert H. A phase I pharmacokinetic and pharmacodynamic study of AT7519, a cyclin-dependent kinase inhibitor in patients with refractory solid tumors. Annals of Oncology, 2011; 22(9): 2137-2143. doi: 10.1093/annonc/mdq734. PMID: 21325451.
25. Gelbert LM, Cai M, Lin X, Sanchez-Martinez, Prado MD, Lallena MJ, Torres R, Rose TA, Wishart GN, Flack RS, Neubauer BL, Young J, Chan EM, Iversen P, Cronier D, Kreklau E, de Dios A. Preclinical characterization of the CDK4/6 inhibitor LY2835219: *in vivo* cell cycle-dependent/independent anti-tumor activities alone/in combination with gemcitabine. Invest New Drugs, 2014; 32(5): 825-37.doi: 10.1007/s10637-014-0120-7. PMID: 24919854.
26. Attwood MM, Fabbro D, Sokolov AV, Knapp S, Schioth HB, Trends in kinase drug discovery: targets, indications and inhibitor design. Nat Rev Drug Discov. 2021; 20(11): 839-861. doi: 10.1038/s41573-021-00252-y. PMID: 34354255.
27. Irie T, Fujii I, Sawa M, Design and combinatorial synthesis of a novel kinase-focused library using click chemistry-based fragment assembly. Bioorg Med Chem Lett. 2012; 22(1): 591-6. doi: 10.1016/j.bmcl.2011.10.076. PMID: 22104147.
28. Zhang J, Yang PL, and Gray NS. Targeting cancer with small molecule kinase inhibitors. Nature Reviews Cancer, 2009; 9(1): 28-39. doi:10.1038/nrc2559. PMID: 19104514.
29. Zhang J, Yang PL, Gray NS. Targeting cancer with small molecule kinase inhibitors. Nat Rev Cancer, 2009; 9(1): 28-39. doi: 10.1038/nrc2559. PMID: 19104514.
30. De Azevedo WF, Leclerc S, Meijer L, Havlicek L, Strnad M, and Kim SH. Inhibition of cyclin-dependent kinases by purine analogues: Crystal structure of human cdk2 complexed with roscovitine. European Journal of Biochemistry, 1997; 243(1-2): 518-526. doi:10.1111/j.1432-1033.1997.00518. x. PMID: 9030780.
31. Wu SY, McNae I, Kontopidis G, McClue SJ, McInnes C, Stewart KJ, Wang S, Zheleva DI, Marriage H, Lane DP, Taylor P, Fischer PM, Walkinshaw MD. Discovery of a novel family of CDK inhibitors with the program LIDAEUS: structural basis for ligand-induced disordering of the activation loop. Structure, 2003; 11(4): 399-410. doi: 10.1016/s0969-2126(03)00060-1. PMID: 12679018.
32. Peng CY, Graves PR, Ogg S, Thoma RS, Byrnes MJ, Wu Z, Stephenson MT, Piwnica-Worms H. C-TAK1 protein kinase phosphorylates human Cdc25C on serine 216 and promotes 14-3-3 protein binding. Cell Growth Differ, 1998; 9(3): 197-208. PMID: 9543386.
33. Copeland RA. The drug-target residence time model: A 10-year retrospective. Nature Reviews Drug Discovery, 2016; 15(2): 87-95. doi:10.1038/nrd.2015.18. PMID: 26678621.
34. Arend KC, Lenarcic EM, Vincent HA, Rashid N, Lazear E, McDonald IM, Gilbert TSK, East MP, Herring LE, Johnson GE, Graves LM, Moorman NJ. Kinome Profiling Identifies Druggable Targets for Novel Human Cytomegalovirus (HCMV) Antivirals. Mol Cell Proteomics, 2017; (4 suppl 1): S263-S276. doi: 10.1074/mcp.M116.065375. PMID: 28237943.
35. Chen Y, Tandon I, Heelan W, Wang Y, Tang W, Hu Q. Proteolysis-Targeting Chimera (PROTAC) Delivery System: Advancing Protein Degraders towards Clinical Translation. Chem Soc Rev, 2022; 51(13): 5330-5350. doi: 10.1039/d1cs00762a. PMID: 35713468.
36. Sliwoski G, Kothiwale S, Meiler J, Lowe Jr EW. Computational methods in drug discovery. Pharmacol Rev, 2013; 66(1): 334-95. doi: 10.1124/pr.112.007336. PMID: 24381236.
37. Wang J, Hou T, Xu X. Recent Advances in Free Energy Calculations with a Combination of Molecular Mechanics and Continuum Models. Current Computer - Aided Drug Design, 2006; 287-306, doi:10.2174/157340906778226454
38. Rohde JM, Brimacombe KR, Liu L, Pacold ME, Yasgar A, Cheff DM, Lee TD, Rai G, Baljinnyam B, Li Z, Simeonov A, Hall MD, Shen M, Sabatini DM, Boxer MB. Discovery and optimization of piperazine-1-thiourea-based human phosphoglycerate dehydrogenase inhibitors. Bioorg Med Chem, 2018; 1; 26(8): 1727-1739. doi: 10.1016/j.bmc.2018.02.016. PMID: 29555419.
39. Pandini A, Fornili A, Fraternali, Kleinjung J. Detection of allosteric signal transmission by information-theoretic analysis of protein dynamics. FASEB J, 2012; 26(2): 868-81. doi: 10.1096/fj.11-190868. PMID: 22071506.
40. Discovery Studio (Version 4.5) [Computer software]. (2022). BIOVIA. https://www.3dsbiovia.com/products/collaborative-science/biovia-discovery-studio/https://www.3dsbiovia.com/products/collaborative-science/biovia-discovery-studio/.
41. Jha V, Devkar S, Gharat K, Kasbe K, Matharoo DK, Pendse S, Bhosale A, Bhargava A, Screening of Phytochemicals as Potential Inhibitors of Breast Cancer using Structure Based Multitargeted Molecular Docking Analysis. Phytomedicine Plus, 2022; 2, 2: 100227. doi: 10.1016/j.phyplu.2022.100227.
42. Kim S, Chen J, Cheng T, Gindulyte A, He J, He S, Li Q, Shoemaker BA, Thiessen PA, Yu B, Zaslavsky L, Zhang J, and Bolton EE. PubChem 2022 update: Improved access to chemical data. Nucleic Acids Research, 2022; 50(D1): D1372-D1381. doi:10.1093/nar/gkab1062. PMID: 30371825.
43. Huang J, Rauscher S, Nawrocki G, Ran T, Feig M, de Groot BL, Grubmüller H, MacKerell AD Jr. CHARMM36m: an improved force field for folded and intrinsically disordered proteins. Nat Methods. 2017; 14(1): 71-73. doi: 10.1038/nmeth.4067. PMID: 27924067.
44. Halgren TA. Merck molecular force field. I. Basis, form, scope, parameterization, and performance of MMFF94. J Comput Chem. 1996; 30; 17(5-6): 490-519. doi: 10.1002/(SICI)1096-987X (199604)17: 5/6<490: AID-JCC1>3.0.CO;2-P.
45. Guedes IA, Costa LSC, Santos KBD, Karl ALM, Rocha GK, Teixeira IM, Galheigo MM, Medeiros V, Krempser E, Custódio FL, Barbosa HJC, Nicolás MF, Dardenne LE. Drug design and repurposing with DockThor-VS web server focusing on SARS-CoV-2 therapeutic targets and their non-synonym variants. Sci Rep, 2021; 11(1): 5543. doi: 10.1038/s41598-021-84700-0. PMID: 33692377.
46. Bray F, Ferlay J, Soerjomataram I, Siegel RL, Torre LA, and Jemal A. Global cancer statistics 2018: GLOBOCAN estimates of incidence and mortality worldwide for 36 cancers in 185 countries. CA: A Cancer Journal for Clinicians, 2018; 68(6): 394-424. doi:10.3322/caac.21492. PMID: 30207593.
47. Malumbres M, and Barbacid M. Cell cycle, CDKs and cancer: A changing paradigm. Nature Reviews Cancer, 2009; 9(3): 153-166. doi:10.1038/nrc2602. PMID: 19238148.
48. Asghar U, Witkiewicz AK, Turner NC, and Knudsen ES. The history and future of targeting cyclin-dependent kinases in cancer therapy. Nature Reviews Drug Discovery, 2015; 14(2): 130-146. doi:10.1038/nrd4504. PMID: 25633797.
49. Horiuchi D, Kusdra L, Huskey NE, Chandriani S, Lenburg ME, Gonzalez-Angulo AM, Creasman KJ, Bazarov AV, Smyth JW, Davis SE, Yaswen P, Mills GB, Esserman LJ, Goga A. MYC pathway activation in triple-negative breast cancer is synthetic lethal with CDK inhibition. J Exp Med, 2012; 9; 209(4): 679-96. doi: 10.1084/jem.20111512. PMID: 22430491.
50. Lim S, and Kaldis P. Cdks, cyclins and CKIs: Roles beyond cell cycle regulation. Development, 2013; 140(15): 3079-3093. doi:10.1242/dev.091744. PMID: 23861057.
51. Sumi NJ, Kuenzi BM, Knezevic CE, Remsing Rix LL, and Rix U. Chemoproteomics reveals novel protein and lipid kinase targets of clinical CDK4/6 inhibitors in lung cancer. ACS Chemical Biology, 2015; 10(12): 2680-2686. doi:10.1021/acschembio.5b00368. PMID: 26390342.
52. Sherr CJ, Beach D, and Shapiro GI. Targeting CDK4 and CDK6: From discovery to therapy. Cancer Discovery, 2016; 6(4): 353-367. doi:10.1158/2159-8290.CD-15-0894. PMID: 26658964.
53. Thomsen R, and Christensen MH. MolDock: A new technique for high-accuracy molecular docking. Journal of Medicinal Chemistry, 2006; 49(11): 3315-3321. doi:10.1021/jm051197e. PMID: 16722650.
54. Friesner RA, Murphy RB, Matthew P Repasky, Leah L Frye, Jeremy R Greenwood, Thomas A Halgren, Paul C Sanschagrin, Daniel T Mainz. Extra precision glide: docking and scoring incorporating a model of hydrophobic enclosure for protein-ligand complexes. J Med Chem, 2006; 49(21): 6177-96. doi: 10.1021/jm051256o. PMID: 17034125.
55. Roe DR, and Cheatham TE. PTRAJ and CPPTRAJ: Software for processing and analysis of molecular dynamics trajectory data. Journal of Chemical Theory and Computation, 2013; 9(7): 3084-3095.doi:10.1021/ct400341p. PMID: 26583988.
56. Daura X, Gademann K, Jaun B, Seebach D, Van Gunsteren WF, and Mark AE. Peptide folding: When simulation meets experiment. Angewandte Chemie International Edition, 1999; 38(1-2): 236-240.doi:10.1002/(SICI)1521-3773(19990115)38: 1/2<236: AID-ANIE236>3.0.CO;2-M.
57. Bharath KC, Shantha KB, Anjana GV, Rajakrishnan R, Ahmed A, Jesu A, Kathiravan MK, S. Karthick RN. Targeting cyclin-dependent kinase 2 CDK2: Insights from molecular docking and dynamics simulation-A systematic computational approach to discover novel cancer therapeutics. Computational Biology and Chemistry,2024; 112: 108134.
58. Schrödinger Release 2021-4: Desmond Molecular Dynamics System, D. E. Shaw Research, New York, NY, 2021. Desmond Maestro-Desmond Interoperability Tools; Schrödinger: New York, NY, 2021.
59. Jorgensen WL. The many roles of computation in drug discovery. Science, 2004; 303(5665): 1813-1818. doi:10.1126/science.1096361. PMID: 15031495.
60. Parry D, Guzi T, Shanahan F, Davis N, Prabhavalkar D, Wiswell D, Seghezzi W, Paruch K, Dwyer MP, Doll R, Nomeir A, Windsor W, Fischmann T, Wang Y, Oft M, Chen T,

Kirschmeier P, Lees EM. Dinaciclib (SCH 727965), a novel and potent cyclin-dependent kinase inhibitor. Mol Cancer Ther, 2010; 9(8): 2344-53. doi: 10.1158/1535-7163. MCT-10-0324. PMID: 20663931.

61. Mita MM, Joy AA, Mita A, Sankhala K, Jou Y-M, Zhang D, Statkevich P, Zhu Y, Yao S-L, Small K, Bannerji R, Shapiro CL. Randomized phase II trial of the cyclin-dependent kinase inhibitor dinaciclib (MK-7965) versus capecitabine in patients with advanced breast cancer. Clin Breast Cancer, 2014; 14(3): 169-76. doi: 10.1016/j.clbc.2013.10.016. PMID: 24393852.
62. Stephenson JJ, Nemunaitis J, Joy AA, Martin JC, Jou YM, Zhang D, Statkevich P, Yao S-L, Zhu Y, Zhou H, Small K, Bannerji R, Edelman MJ. Randomized phase 2 study of the cyclin-dependent kinase inhibitor dinaciclib (MK-7965) versus erlotinib in patients with non-small cell lung cancer. Lung Cancer, 2014; 83(2): 219-223. doi: 10.1016/j.lungcan.2013.11.020. PMID: 24388167.
63. Asghar US, Barr AR, Cutts R, Beaney M, Babina I, Sampath D, Giltnane J, Lacap JA, Crocker L, Young A, Pearson A, Herrera-Abreu MT, Bakal C, Turner NCC. Single-Cell Dynamics Determines Response to CDK4/6 Inhibition in Triple-Negative Breast Cancer. Clin Cancer Res, 2017; 23(18): 5561-5572. doi: 10.1158/1078-0432.CCR-17-0369. PMID: 28606920.
64. Bose P, Simmons GL, and Grant S. Cyclin-dependent kinase inhibitor therapy for hematologic malignancies. Expert Opinion on Investigational Drugs, 2013; 22(6): 723-738. doi:10.1517/13543784.2013.789859. PMID: 23647051.
65. Newcomb EW, Tamasdan C, Entzminger Y, Arena E, Schnee T, Kim M, Crisan D, Lukyanov Y, Miller DC, Zagzag D. Flavopiridol inhibits the growth of glioma cells indirectly by targeting the p65 subunit of NF-κB. Journal of Neuro-oncology, 2023; 61(3): 193-202. doi:10.1023/A:1026113321156.
66. Byrd JC, Lin TS, Dalton JT, Wu D, Phelps MA, Fischer B, Moran M, Blum KA, Rovin B, Brooker-McEldowney M, Broering S, Schaaf LJ, Johnson AJ, Lucas DM, Heerema NA, Lozanski G, Young DC, Suarez J-R, Colevas AD, Grever MR. Flavopiridol administered using a pharmacologically derived schedule is associated with marked clinical efficacy in refractory, genetically high-risk chronic lymphocytic leukemia. Blood, 2007; 109(2): 399-404. doi: 10.1182/blood-2006-05-020735. PMID: 17003373.
67. Finn RS, Martin M, Rugo HS, Jones S, Im S-A, Gelmon K, Harbeck N, Lipatov ON, Walshe JM, Moulder S, Gauthier E, Lu DR, Randolph S, Diéras V, Slamon DJ. Palbociclib and Letrozole in Advanced Breast Cancer. N Engl J Med, 2016; 375(20): 1925-1936. doi: 10.1056/NEJMoa1607303. PMID: 27959613.
68. Cristofanilli M, Turner NC, Bondarenko I, Ro J, Im S-A, Masuda N, Colleoni M, DeMichele A, Loi S, Verma S, Iwata H, Harbeck N, Zhang K, Theall KP, Jiang Y, Bartlett CH, Koehler M, Slamon D. Fulvestrant plus palbociclib versus fulvestrant plus placebo for treatment of hormone-receptor-positive, HER2-negative metastatic breast cancer that progressed on previous endocrine therapy (PALOMA-3): final analysis of the multicentre, double-blind, phase 3 randomised controlled trial. Lancet Oncol, 2016; 7(4): 425-439. doi: 10.1016/S1470-2045(15)00613-0. PMID: 26947331.
69. Chen R, Keating MJ, Gandhi V, and Plunkett W. Transcription inhibition by flavopiridol: Mechanism of chronic lymphocytic leukemia cell death. Blood, 2005; 106(7): 2513-2519. doi:10.1182/blood-2005-04-1678. PMID: 15972445.
70. Ghose AK, Herbertz T, Pippin DA, Salvino JM, and Mallamo JP. Knowledge-based prediction of ligand binding modes and rational inhibitor design for kinase drug discovery. Journal of Medicinal Chemistry, 2012; 55(15): 6552-6562.doi:10.1021/jm300361f. PMID: 18710211.

Cite this article: Aloqbi AA. *In silico* and *In vitro* Characterization of Potent CDK2 Inhibitors as Probable Cancer Therapeutics. Indian J of Pharmaceutical Education and Research. 2025;59(4):1582-602.